GEORG-AUGUST-UNIVERSITÄT
GÖTTINGEN

Fakultät für
Physik

Bachelor's Thesis

Measurement of Operational Stability of the ATLAS Pixel Read-Out Chip at low Threshold

Messung des stabilen Arbeitsbereichs des ATLAS Pixel Auslesechips bei niedrigen Schwellen

prepared by

Julia Rieger

from Hann. Münden

at the II. Physikalisches Institut - Atom- und Teilchenphysik

Thesis period:	12th April 2010 until 23rd July 2010
First Referee:	PD Dr. Jörn Große-Knetter
Second Referee:	Prof. Dr. Arnulf Quadt
Thesis Number:	II.Physik-UniGö-BSc-2010/09

Contents

1 Introduction

The world is made out of matter. Thus it is obvious, that scientists are interested for centuries in the structure of matter. Today the fundamental structure is described by the *Standard Model* of particle physics. It contains three different components. Firstly matter particles, leptons and quarks, secondly interaction particles which describe the three different forces, electromagnetic, weak and strong interaction. Finally, the Higgs particle is included in this model. It is the only particle of this theory that is not discovered yet.
The Standard Model is one of the best tested theories and its predictions come to a very precise agreement with measurements. With the construction of the *Large Hardron Collider* (LHC) physicists hope to find new physics, because of the access to higher energy regions.
The LHC is located at the *European Organization for Nuclear Research* (CERN) and is the highest-energy particle accelerator. It is designed to collide bunches of protons, where every bunch consists of 10^{11} protons. The first collision took place in 2009 with a centre-of-mass energy of 900 GeV. This will be increased up to 14 TeV in the next years.
The *ATLAS Detector* is one of four experiments which are operated at LHC. Its intentions are to find the Higgs particle, if it exists, to collect precise data for the Standard Model and to find physics beyond the Standard Model.
The detector consists of four major components. The innermost is a tracking system, which measures the momentum of each charged particle. In the middle there is a calorimeter system to measure the energy of the particles. The outermost component is a muon detection system. Furthermore, there is the magnet system with a magnet that creates a solenoidal field of 2 T and a toroid system with eight coils that generates a peak field of about 4 T. The fields are used to bend the tracks of charged particles for the momentum measurement.

The LHC is designed to achieve a luminosity of 10^{34} cm^{-2} s^{-1}. After a few years

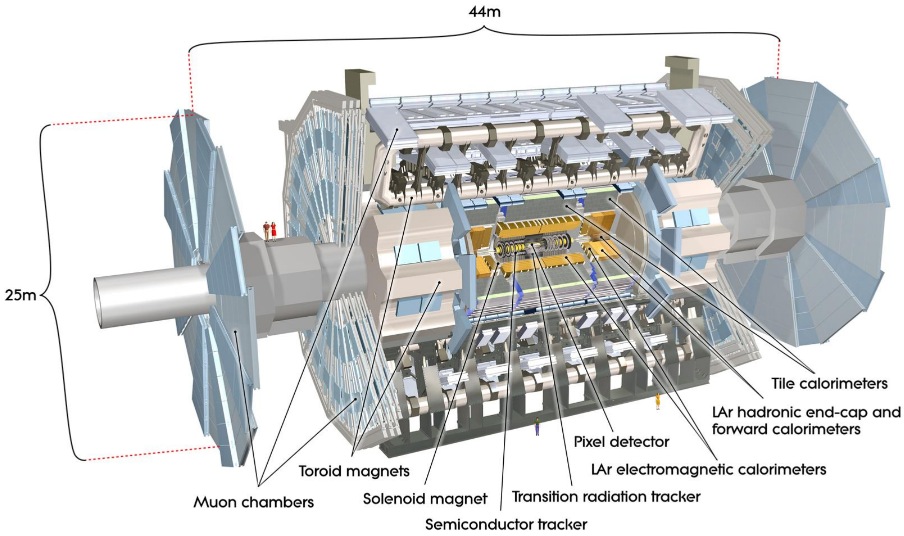

Figure 1.1: Schematic view of the ATLAS detector [1].

of data taking it is planned to increase the luminosity to 10^{35} cm^{-2} s^{-1} with the upgrade of the LHC to *Super Large Hadron Collider* (SLHC) [2].

With this upgrade the particle flux through the detector layers is increased by approximately a factor ten due to the increase in luminosity. Particularly in the innermost part of the ATLAS Detector, the *ATLAS Pixel Detector*, the radiation dose will be very high.

In Chapter 2 the Pixel Detector will be introduced with a special focus on the effects on the sensor due to radiation damage and the read-out system. The sensors will not be able to stand this radiation for long time. The main focus of the irradiation studies is the fact that the signal from the particles decreases. Thus hits by particles might get lost. One possible modification is to decrese the threshold of the read-out system.

The test system which was used during the thesis and the used methods and problems are described in Chapter 3. One aspect is to minimise the operational threshold for the read-out system. Therefore a method for the measurement of the minimum threshold has been developed (Chapter 4). Chapter 5 deals with the variation of read-out chip parameters and configurations which could influence the minimum threshold.

2 The ATLAS Pixel Detector

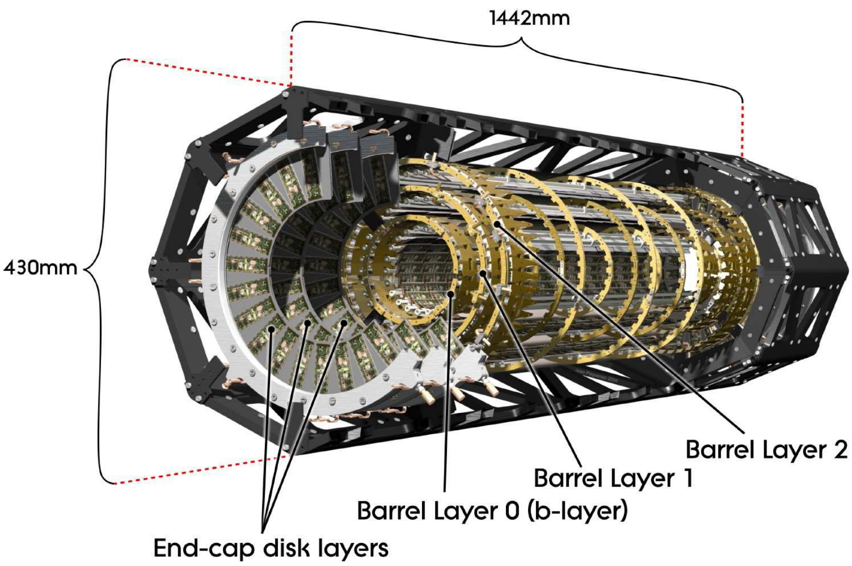

Figure 2.1: A schematic view of the pixel detector consisting of barrel and endcap layers [3].

This thesis will concentrate on the Pixel Detector, which is the innermost component needed for track and vertex reconstruction and b-tagging. It is divided into three barrel-shaped layers and three disks on each side.

The Pixel Detector faces the highest particle flux due to the position closest to the beam pipe. The annual fluence for the innermost barrel layer is $25 \cdot 10^{13}$ cm^{-2}.

The main detector components are 1744 sensor-chip-hybrid modules. One of these modules consists of a sensor with 47232 pixels, which are connected to 16 front-end (FE) chips using bump bonding technique. This corresponds to approximately $8 \cdot 10^7$ pixels on all modules, each has a size of 50 μm $\times$ 400 μm [4]. There is a total active area of about 1.7 m^2.

2.1 The Sensor

2.1.1 Signal Generation in Semiconductors

The sensor is the sensitive part of the pixel detector. If a charged particle penetrates the silicon the main process of losing energy is ionisation, where electron-hole pairs are produced. The amount of energy lost per distance is described by the Bethe-Bloch formula [5]

$$-\langle\frac{\mathrm{d}E}{\mathrm{d}x}\rangle = 2\pi N_A r_e^2 m_e c^2 \rho \frac{Z}{A}\frac{z^2}{\beta^2}\left\{\ln\left(\frac{2m_e c^2\beta^2\gamma^2 W_{\max}}{I^2}\right) - 2\beta^2 - \delta - 2\frac{C}{Z}\right\},$$

where r_e is the classical electron radius, m_e the electron mass, N_A Avogadro's number, I the mean excitation potential, Z the atomic number of the absorbing material, A atomic weight of absorbing material, ρ the density of the absorbing material, z the charge of an incident particle in units of e , δ the density correction, C the shell correction and finally the maximum energy transfer $W_{\max}$ in a single collision.
The formula has a minimum at $\beta\gamma = 3.5$ which corresponds to an energy loss of $\langle\frac{\mathrm{d}E}{\mathrm{d}x}\rangle \approx 1.5\frac{\mathrm{MeV}}{\mathrm{g\ cm^{-2}}}$. Particles with this energy loss are called minimum ionizing particles (m.i.p.).
The sensor used in the Pixel Detector has a thickness of 250 μm. If the density of the sensor material and the energy for producing an electron-hole pair is considered a m.i.p., which passes the sensor vertically, a signal of about 24000 e is expected.
In order to detect this charge, the sensor has to be depleted and an external field is needed to separate the two charge carrier types. The drifting charges induce a signal on the read-out electrodes.

2.1.2 Radiation Damage

Irradiation damages the sensor. There are two categories, non-ionising energy loss, which affects mainly the bulk material, and ionising energy loss, affecting the surface of the sensor.
The non-ionising energy loss is mainly caused by heavy particles (no $e^{\pm}$, γ). There are collisions with the atoms in the crystal lattice. These atoms are knocked out of the lattice and can remove secondary atoms from the lattice creating cluster defects. New states in the band-model of the semiconductor are created due to the cluster defects. According to the position of the gaps this can cause different effects.

There can be trapping centres which catch free charge carriers. This leads to a decrease in signal charge. After irradiation of an ATLAS life-time dose there are only 10000 e - 15000 e expected for a m.i.p.. Furthermore, due to the acceptor-like defects the effective doping concentration is changed. This affects the depletion depth of the material and causes type inversion from n-type to p-type. In addition there can be generation and recombination centres. The electron-hole pairs can recombine easier and there is more thermal excitation. Thus there is a higher leakage current. Therefore the sensor needs to be cooled.

2.1.3 Sensor Design

The sensor consists of oxygenated silicon n-type bulk material with n^+ pixel implants. Because the sensor material needs to be radiation hard, the silicon is oxygenated. With oxygenated silicon the depletion voltage does not have to be increased as strongly as if for standard silicon.
Due to radiation damage the effective doping concentration is changed. For unirradiated sensors, the depletion starts at the back side. Thus the pixels are not isolated from each other until full depletion of the bulk. After the type inversion the depletion starts from the pixels, so that the sensor can work even if the sensor is not completely depleted (see Figure 2.2). In order to maximize the signal, it is desirable to deplete a region as much as possible.

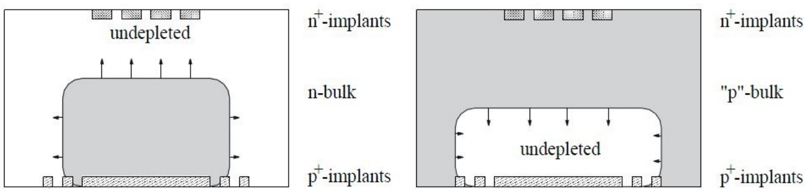

Figure 2.2: Schematic view of the development of the depletion region before (left) and after (right) type-inversion [4].

The size of the pixels is determined by the expected occupancy, the space for the electronics and the maximal required spatial resolution. According to this the resolution of the ATLAS Pixel Detector is about 12 μm in azimuth and about 115 μm parallel to the beam pipe [4]. Because collisions are expected every 25 ns (40 MHz) the detector needs a high read-out speed. On account of this, every pixel has its own read-out circuit. The read-out chips are connected via bump bonds on the back of the sensor. Overall there are 80 million read out channels instrumented.

There are four different types of pixels due to the gaps between adjacent front-end chips. The normal pixels have a size of 50 μm $\times$ 400 μm. To cover the gaps there are long pixels of 50 μm in $R\phi$ by 600 μm in Z. In the middle of a module there is a gap between the FE chips. There are eight pixels, four for every FE chip, which are not directly connected to a FE chip. These pixels are connected to pixels with own FE chips, which have then two inputs. Both pixel types are called ganged pixels. The pixels between the ganged pixels are called inter-ganged pixels. The described layout can be seen in Figure 2.3.

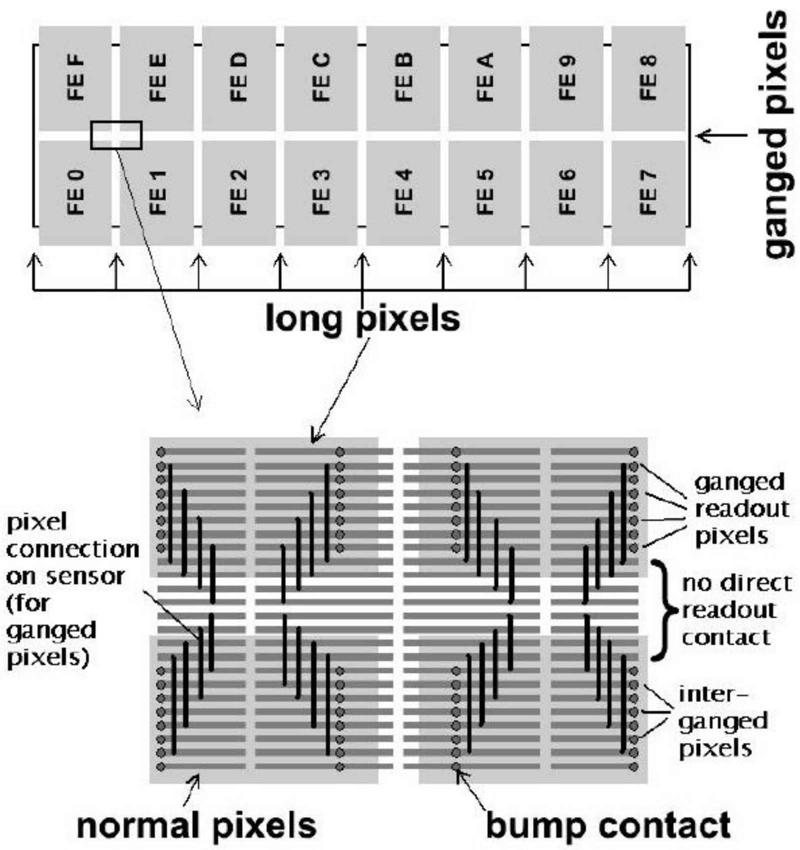

Figure 2.3: Schematic drawing of the different pixel types [4].

2.2 The Front-End Chip

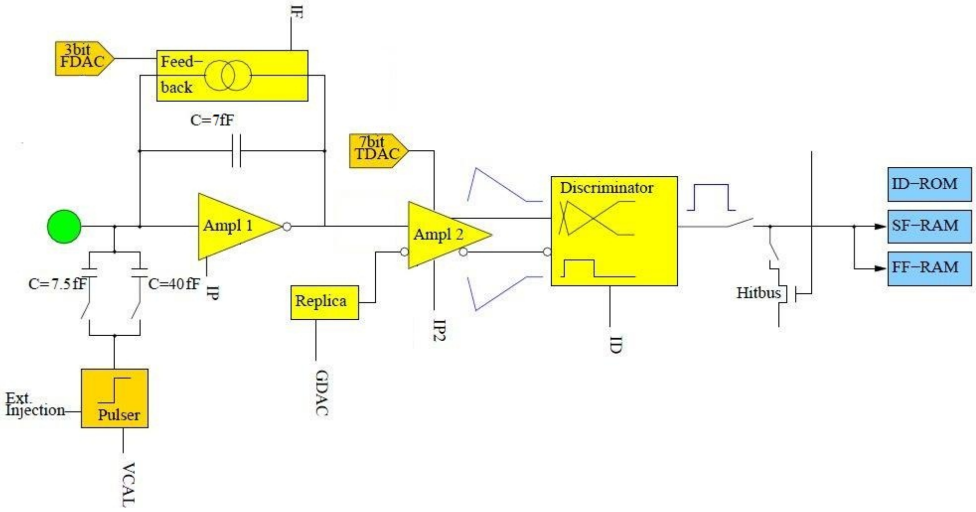

Figure 2.4: Schematic view of a pixel unit cell [7].

The FE chip digitizes signal charge from the sensor. Every FE chip consists of 2880 analogue circuits with a digital read-out that operates at 40 MHz clock, synchronized with the LHC clock [6]. The channels are arranged in an 18×160 matrix. Two columns are combined into a pair for digital read-out.

The analogue and the digital circuit have separate supply voltages. For the digital part it is $V_{DD} = 2.1$ V and for the analogue part $V_{DDA} = 1.7$ V.

The analogue part contains a fast preamplifier and a DC-coupled second amplifier. The preamplifier integrates the induced charge of the sensor using a feedback capacitor, which is discharged by a constant feedback current I_F. This current can be set by a global 8-bit DAC [1] or individually using the 3-bit feedback DAC (FDAC). The outgoing signal is amplified in a second stage differentially. Therefore the amplifier needs a second signal. This comes from a replica circuit which reproduces the DC potential of the first amplifier part [7]. Both amplifiers need a supply current I_P respectively I_{P2}.

Subsequently comes the discriminator which needs the current I_D. The main principle of a discriminator is that it compares an adjustable threshold with an input signal. If the signal is higher than the threshold, the output is a logical one, otherwise it is zero.

[1]DAC=Digital to Analogue Converter

For the rising and falling edge of the logical one a time stamp is stored into a RAM[2]. For every double column there is a shared bus, which stores the hit signal in the buffer at the end of the column, named End-of-Column-Logic (EoC).
Additionally the signal is fed into a hitbus. This is an OR gate which goes to logical one if there is a hit in one of the 2880 pixels.

A global 5-bit DAC (GDAC) is used to set the threshold for a whole FE chip. Another way to set the threshold for every single pixel is the 7-bit TDAC, which is required to compensate differences between the pixels.

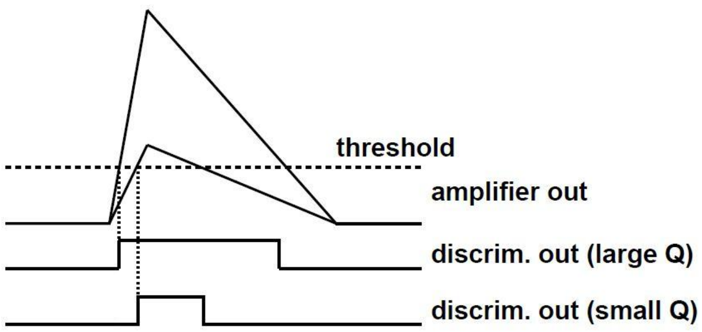

Figure 2.5: Amplifier output and discriminator response for different feedback currents [4].

In Figure 2.5 the translation from the analogue information of the incoming pulse into the length of the digital signal is shown. The time during which there is logical one is called time over threshold (ToT). The ToT is proportional to the induced charge, because of the constant discharging current. It is measured in clock cycles of 25 ns length. The difference between the rising and the falling edge of the digital signal is derived in the EoC-logic and produces the ToT.

During the thesis I took a closer look at the threshold. The standard value for the threshold is about 4000 e, which is needed to suppress noise hits, which have a magnitude of about 200 e. The expected signal from a m.i.p. particle in the detector is as derived above at about 24,000 e.
In order to test a FE chip, the possibility to inject charge directly into the preampli-

[2]RAM: Random-Access-Memory

fier (analogue injection) or the discriminator (digital injection) exists. This charge is generated by applying a voltage pulse to a capacitor. The amplitude is controlled by a DAC, called VCAL. Two different capacitors can be selected C_{low} and C_{high}, which have a standard value of about 7.5 fF and 40 fF, respectively.

3 Measurements - Methods and Setup

3.1 Test System

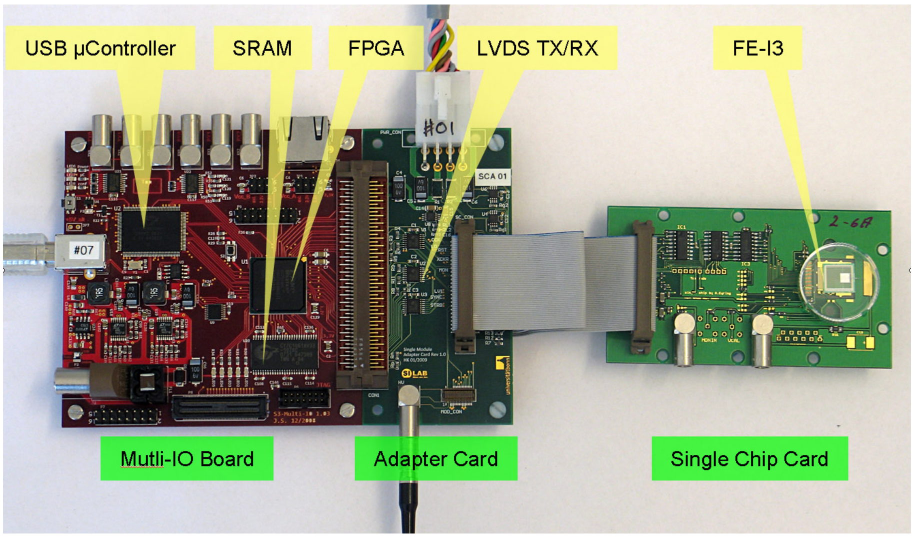

Figure 3.1: UBSPix board with single chip card [9].

The USBPix system (see Figure 3.1) is used in order to test a FE-I3 single chip with and without a sensor. It contains a SiLab[1] multi purpose IO-board (S3MultiIO) with a USB2.0 interface to a PC and an adapter card which connects the S3MultiIO to the Single Chip Adapter Card. The latter houses the FE-I3 chip. Furthermore, the high voltage is applied using a LEMO connector.
The S3MultiIO contains a micro controller, a Field Programmable Gate Array (FPGA), a Static Random Access Memory (SRAM) and several LEMO inputs and outputs. It is powered by the USB connector. The micro controller can initialize all

[1]Universität Bonn

operation loops for the needed scans. The FPGA provides and handles all signals going to the FE, like configuration and charge injection, and stores data coming from the FE in the SRAM. Thus threshold scans (see Section 3.2) can be done without communication to the PC, only by the USBPix system itself [8].

STcontrol is the user interface to configure and operate the system. The application software for the USBPix system can be changed by a C++ code collection called ATLAS PixLib package. STcontrol provides the chip configurations, includes different tests and measurements and has a data analysis tool called Module Analysis attached.

3.2 Threshold Scan

To decrease the threshold it needs to be measured first. Therefore the software has an algorithm, called threshold scan.
During this scan a charge is injected into the preamplifier. This process is repeated multiple times. Then the value of the injected charge is increased in discrete voltage steps controlled by VCAL. The process is repeated until a specified range is reached. The number of charge injections at each charge value corresponds to the number of events per scan point.

If there was no noise, the occupancy versus the injected charge would be a step function. No hits would be produced by injections below the threshold and all injections above the threshold would result in a hit.
But there is noise from the analogue part and the digital crosstalk. Thus the hit probability p_{hit} [4] is given by an error function

$$p_{\mathrm{hit}}(Q) = \frac{1}{2}\mathrm{Erfc}\left(\frac{Q_{\mathrm{thresh}} - Q}{\sqrt{2}\sigma_{\mathrm{noise}}}\right),$$

where Q, the charge of the injected pulse, is given in DAC units, Q_{thresh} is the charge which corresponds to the discriminator threshold and σ_{noise} is the equivalent noise charge (ENC) of the detector-amplifier system. Erfc is the complementary error function defined by $\mathrm{Erfc}(x) = 2\int_x^\infty e^{-x'^2}\mathrm{d}x'/\sqrt{\pi}$. This function is referred to as S-curve.

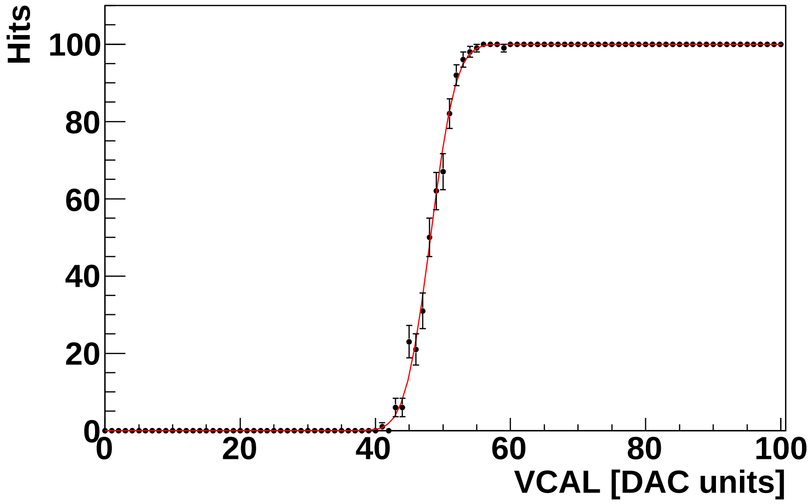

Figure 3.2: Hits versus VCal, which corresponds to the injected charge.

Figure 3.2 shows an example of a threshold fit with an S-curve. Each charge value was injected 100 times. The values of this fit are recorded as the threshold Q_{thresh} and noise σ_{noise}, for each pixel and stored in histograms.
Thus the threshold scan produces three different histograms (see Figure 3.3) titled SCURVE_MEAN, which shows the different thresholds of all pixels, SCURVE_SIGMA, which shows the noise for the pixels, and SCURVE_CHI2, which shows the χ^2. These three histograms have a certain width, which represents the difference in the values between the single pixels.

3.3 Sources of Noise

3.3.1 Noise in Analogue Electronics

In the analogue part of the sensor the three main sources of noise are:

- **Shot noise**
  Shot noise in electronics is generated by random fluctuations of the electric current in an electrical conductor. The current is carried by discrete charges. The result is shot noise at the input of the amplifier. This noise can only appear if a current is generated.

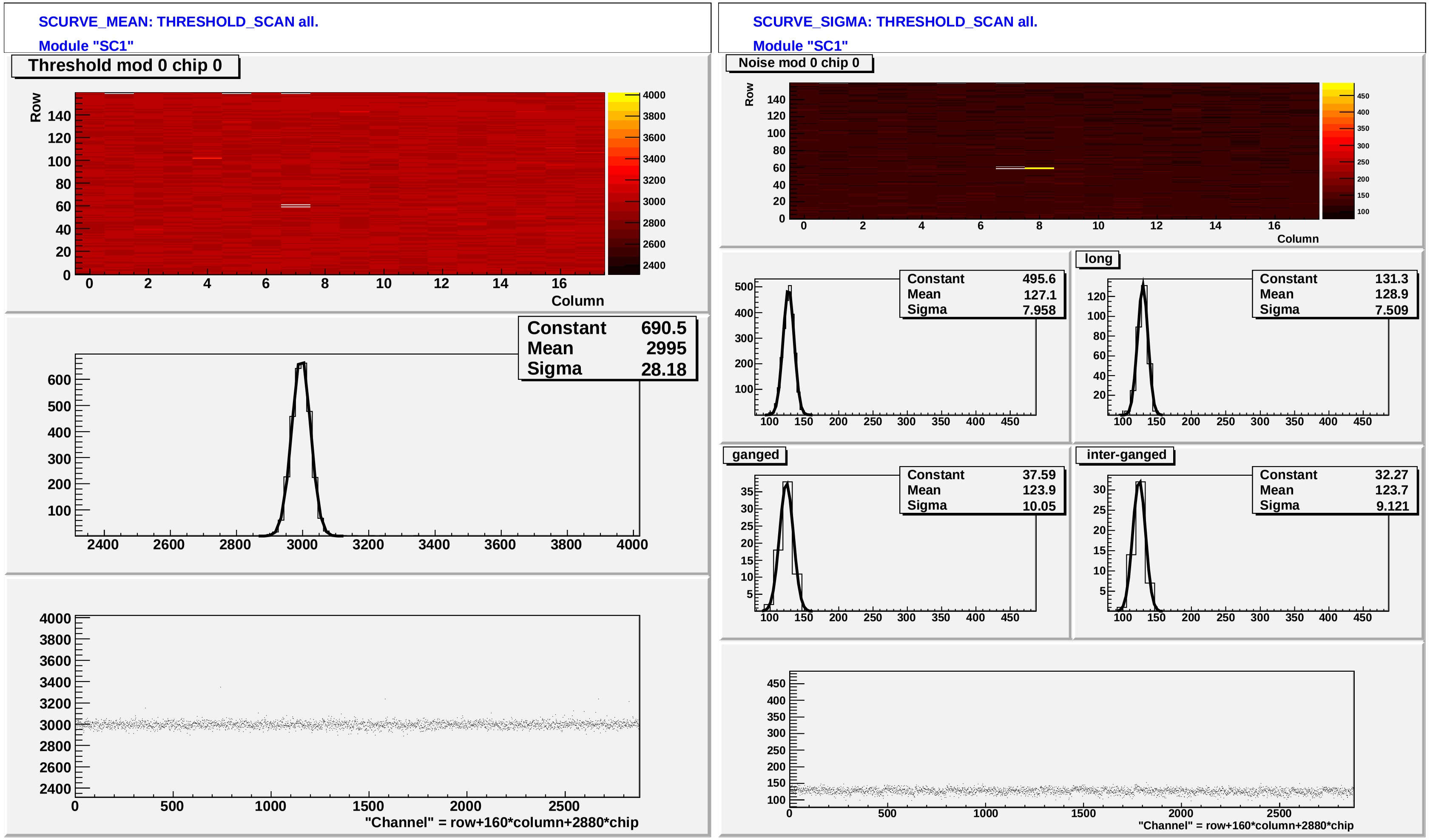

Figure 3.3: Example for the output of a threshold scan for a chip without sensor; Distribution of the threshold (left) and of the noise for the different pixel types(right);
Colour-coded 2D map of the chip (top), projection of the values (middle) and scatter plot (bottom).

- **Thermal noise**
  Thermal noise is caused by the random thermal motion of charge carriers inside an electrical conductor. This happens regardless of any applied voltage.

- **$1/f$ noise**
  $1/f$ noise occurs in almost all electronic devices and results from a variety of effects, though always related to a direct current. Unlike shot and thermal noise the $1/f$ noise depends on the frequency.

3.3.2 Digital Crosstalk

Empirically, it was found that the pixels of a chip tend to get into an unstable condition if the threshold becomes too low. The reason is a larger digital activity, because there can be more noise hits.
The FE chip has a mixture of analogue and a digital circuitry. Digital crosstalk between these circuits can happen through the bulk material of the chip. The state of the digital circuits changes between logic one and logic zero. If many circuits change their state at the same time there is a voltage drop in the supply line. Through capacitances of the bulk material, the voltage drop can cause charge injections into the bulk material [10]. This charge generates noise and more noise hits. Then there is even more activity and the digital crosstalk increases again. If the threshold is too low, in almost all pixels a hit can be seen. This activity is too much for the read-out and the chip stops working.

There is a second type of crosstalk in the analogue part. Analogue crosstalk is the charge that has to be injected into a neighbouring pixel in order to fire a reference pixel. It is given as the ratio of the injected charge into the neighbour pixel divided by the threshold of the reference pixel [11]. But this type causes only a small effect.

3.4 Effects at Low Thresholds

As mentioned in Section 2.1.2 the signal charge is reduced to 10000 e - 15000 e for a m.i.p. due to radiation damage. If this charge is injected into only one pixel a threshold of 4000 e is low enough to detect the signal. But most of the times, the hit is shared by several pixels. If a signal charge of 10000 e is distributed to three pixels, the signal is below the threshold and the hit gets lost.

This is a reason why the threshold has to be decreased. But there are some problems at low thresholds. If the threshold gets too low, there is more activity on the chip due to noise. The digital crosstalk increases and the chip has an unstable behaviour. Thus the threshold cannot be estimated reliably, because the digital crosstalk can not be calculated.

The main intention of this thesis is to determine the minimum threshold at which the FE chip can be operated stably and to decrease the stable minimum threshold by varying several parameters and adjustments of the chip.

4 Minimum Threshold Measurements

At first, a measurement for the minimum threshold had to be developed, which operates stably and is reproducible. During the thesis three different options were tested and partly improved, a hitbus method, a TDAC tune method and the incremental TDAC scan method, which will be explained in the following sections.

4.1 Hitbus Measurement

As described, the hitbus is an OR that gives a logical one if a hit is seen in the sensor. At a standard threshold (e.g. 4000 e) the chip without a sensor is supposed to see no hits, if no charge is injected. If there is a sensor on the chip, there are hits caused by cosmic muons. These muons are produced by interactions of the cosmic rays with the atmosphere. About 10,000 muons reach every square meter of the earth's surface a minute. Thus the sensor should see about 1-2 muons per minute.

The USBPix system has the possibility to send the hitbus signal to one of the LEMO connectors. This connector is wired to a counter. The idea is to count the hits, which are seen by the hitbus, for a given time period, while decreasing the TDAC step by step, which decreases the threshold. Before the scan starts the chip is tuned to a standard threshold.
At first, there should be only hits by the muons for chips with sensor or no hits for a long time period (100 min) for chips without a sensor. If the threshold decreases the number of hits increases because the chip comes to the critical behaviour.

In Figure 4.1 one example of a measurement for a chip with sensor is shown. The hitbus rate was converted into the occupancy using the relation

$$\text{occupancy} = \frac{\#\text{hits / time}}{25\ \text{ns} \cdot 2880\ \text{pixel}}.$$

For higher thresholds, the occupancy is low. At about 3200 e the occupancy increases. At some point, the amount of hits caused by digital crosstalk becomes too large and the chip sees no hits at all.
Unfortunately, the number of hits changes, even for the same configurations. Figure 4.1 shows that the values vary even for the same threshold. The points were measured on two different days. This was investigated more precisely.
The conclusion was that this method is not stable enough to make reliable measurements. It depends on different external parameters like electromagnetic pick-up, ripples on the buildings power nets, temperature etc.

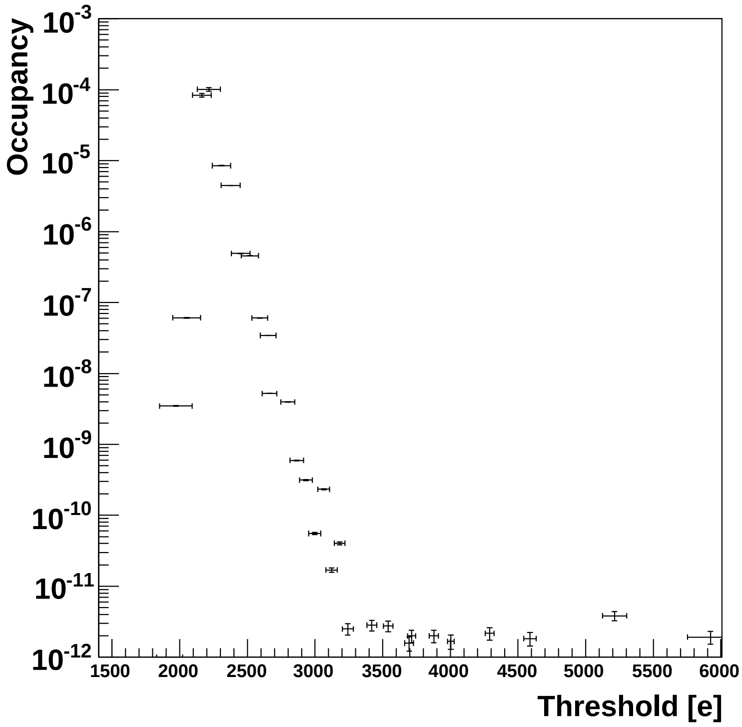

Figure 4.1: Occupancy versus threshold from the hitbus measurement with sensor.

4.2 TDAC Tune

As mentioned before, the TDAC is a 7-bit digital-to-analogue converter. It determines the fine-adjustment of threshold values for each pixel. To tune the TDAC of each pixel to a desired threshold the TDAC tune is used. This is a measurement provided by STcontrol.
A charge which corresponds to the desired threshold is injected into the preamplifier on the front-end chip. If the injected charge is above the threshold the result is a hit. The injection is repeated several times per scan point. If the percentage of injections causing a hit is below 50 % the TDAC is decreased by a step size that can be set. If the percentage is above 50 % the TDAC is increased. The TDAC settings after a specified number of iterations is stored in a TDAC map [12].
Using this map a threshold scan can be made. The TDAC tune works very well for standard threshold (around 4000 e). If the desired threshold is below 2500 e the tune stops working as desired. Next to the main peak in the threshold distribution there is a smaller peak at higher thresholds (at about 3000 e with a height of 100 hits).
The general steps, starting from TDAC=70 DU[1] for all pixels, is 16, 8, 4, 2, 1, 1. The lowest possible TDAC value with this setting is TDAC=38 DU. For lower thresholds the start value of the scan has to be set. If the first step is too large the TDAC becomes too small and the chip does not work properly. Because of this, no hits are registered and the TDAC is decreased again. If the starting point is chosen carefully and the step size is decreased, e.g. step sizes of only one DU, the scan can be improved. The scan operates down to a threshold of about 2000 e but there are always some pixels that have a threshold beyond the dispersion of the pixel. Another disadvantage is that the start point has to be set. Therefore the relation between TDAC and threshold must be known.
The minimum threshold is determined by looking at the threshold scan with the tuned configuration. If the S-curve fit still works the threshold of the TDAC tune can be decreased. Another TDAC tuning with a lower desired threshold is made. At some point the threshold scan stops working. Close to this point there is the minimum threshold.
This method is not reliable enough because it depends on the start parameter and it is not stable enough.

[1] DU: DAC units

A different modification of this method was tested. A TDAC tuning is made for a threshold where the scan works properly. Afterwards the TDAC distribution is stored but all TDAC values are decreased step by step until the minimum threshold is reached. There is the problem that the noise increases above 500 e for some pixels. The distribution gets smeared out.

4.3 Incremental TDAC Scan

The incremental TDAC scan is supposed to find a TDAC distribution which corresponds to the minimum operating threshold. This scan was already included in the PixLib package, but did not find the minimum threshold. During the thesis this was improved.
The idea behind this scan is to decrease the TDAC for every pixel individually and to check after every step if the S-curve fit (see Section 3.2) still works. At the beginning of the scan the TDAC values are distributed like for a standard threshold (3000 e - 4000 e). At first, the scan decreases the TDAC values by five DU steps. If the fit fails, the TDAC is increased by five DU again. Afterwards the step size is reduced by one DU and the TDAC is decreased again by four DU. Then a new threshold scan follows.
An important component of this scan is the decision at which conditions the fit fails. The exclusion conditions, which say that the fit failed, are:

- The mean value of the threshold Q_{thresh}: $Q_{\mathrm{thresh}}<1$ e and $Q_{\mathrm{thresh}}>15000$ e
- The mean value of the χ^2: $\chi^2<1$ and $\chi^2>50$
- The mean value of noise σ_{noise}: $\sigma_{\mathrm{noise}}<1$ e and $\sigma_{\mathrm{noise}}>$noisecut

It has to be mentioned that the cut on the χ^2 does not affect the scan, because at the state of the thesis, the χ^2 calculation did not work properly.
The noisecut is the most important cut. For a chip without a sensor it is noisecut=200 e. For a chip with a sensor there are four types of pixels with different noise. The noise changes if different chips are used. The choice for the used chip can be seen in Table 4.1. For the choice of this values the noise values of a threshold scan with a standard threshold were estimated. The cut is where there are no more entries in the histogram.

Pixel Type	normal	long	ganged	inter-ganged
Cut [e]	225	250	400	250

Table 4.1: Noise cuts for the chip with sensor.

The scan produces a TDAC map. For a better stability all TDACs have to be increased after the scan by one DU. A threshold scan gives then the minimum threshold.
The incremental TDAC scan was the most reliable method to find a reproducible minimum threshold. It is used for the following measurements.

In order to test the method, the correlation of two different minimum threshold scans was considered. Correlations are useful because they can indicate a predictive relationship. If the correlation coefficient is close to 1, the two quantities have a positive linear relation. If it is -1, the relation is negative linear. The quantities are independent if there is a correlation of 0.
It is expected that the correlation of two successive minimum threshold scans is almost 1. The correlation coefficient for two standard threshold scans is between 0.7 and 0.8. This shows that the threshold scans give the same results. The threshold values of the single pixels are reproducible.
For the measurements of the minimum threshold for a chip without sensor and with sensor the mean value of the correlation coefficients can be seen in Table 4.2. Therefore four measurements of the minimum threshold with the same configurations without sensor, respectively five measurements with sensor were made. With these measurements the correlation coefficient was caculated.

chip	correlation coefficient
without sensor	0.13 ± 0.07
with senosr	0.33 ± 0.03

Table 4.2: Correlation coefficients between two the incremental TDAC scans.

The correlation coefficients between two incremental TDAC scans are low. This indicates that the individual threshold values for the single pixels are not reproducible. But the mean value is reproducible which will be shown in later measurements.

Thus the low correlation coefficients seem not to influence the measurement, but there might be a collective behaviour of the single read-out channels.

5 Different Approaches to the Minimum Threshold

In order to find an operation point, at which the minimum threshold is decreased, different parameters like the supply voltage and amplifier currents are varied. Furthermore connections between the grounds and the mask steps are changed.
The measurements are done with the incremental TDAC scan. The start configuration is always the same. The standard configuration is shown in Table 5.1.

V_{DD}	V_{DDA}	GDAC	I_F	I_P	I_{P2}	I_D
2.1 V	1.7 V	8/16* DU	30 DU	64 DU	64 DU	64 DU

Table 5.1: Standard configuration for all scans.

During the measurements only one parameter is changed at a time and the others stay at the standard values. The bias voltage for the sensor is $U_{\mathrm{dep}} = -150$ V.
The first observation is that there is a difference if there is a sensor on the chip or not. The minimum threshold without a sensor is 1547 ± 28 e and with sensor is 1892 ± 54 e. These mean values and standard deviations are estimated from 12 measurements with the same configurations at different times.

5.1 Supply Voltages

One pixel contains an analogue and a digital circuit. Both have separate supply voltages. It must be pointed out that the digital supply voltage V_{DD} is at all times larger than the analogue supply voltage V_{DDA}. If the voltages are too low the chip will not work. This happens at a digital voltage of about 1.6 V. The voltage should not be larger than 2.5 V to avoid damages of the chip.

*without/with sensor

At first measurements without a sensor on the chip are examined. In Figure 5.1 the dependency of the minimum threshold on the analogue voltage V_{DDA} is shown. The data are fitted with a constant function. This description is obviously not good.
If the points in figure 5.1 are regarded it looks like fluctuations around the constant. It must be pointed out that the errors for the data are calculated for the measurement with the standard configuration. Thus the errors can be underestimated or they can change with the voltage. Furthermore, it has to be taken into account that there are correlations between the threshold and the supply voltage. In different parts of the chip reference voltages are generated out of the supply voltages.

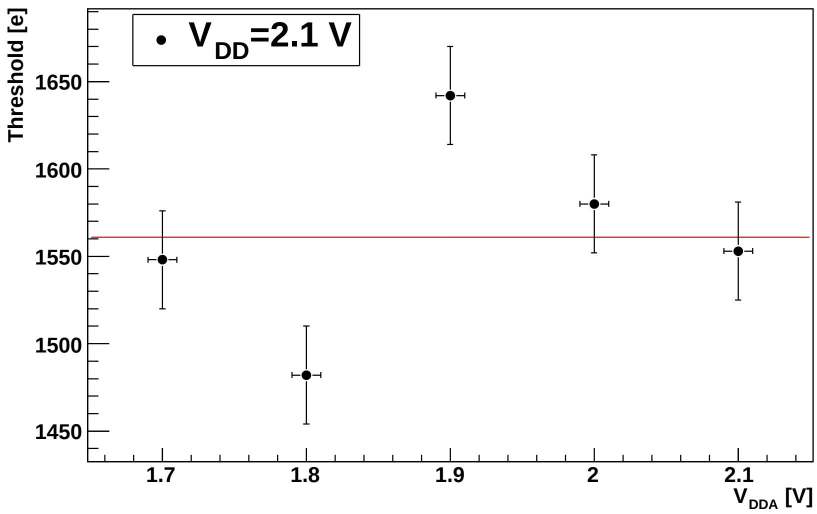

Figure 5.1: Dependency of the minimum threshold on the analogue voltage V_{DDA} without sensor.

Figure 5.2 shows the dependency of the minimum threshold on the digital voltage V_{DD}. The minimum threshold increases with the digital voltage. With an increase of the digital voltage there is a larger difference between the logic level. Thus the digital crosstalk increases.
There is a peak at 1.86 V. To estimate where the peak comes from the conditions why the incremental TDAC scan stopped were investigated. At the last scan point of the scan the noise of the chip with V_{DD}=1.8 V is higher. The reason for the failure of the fit at V_{DD}=2.1 V was that the noise was at 200 e - 400 e. At V_{DD}=1.8 V the fit failed because the noise was 1000 e or higher. There seems to be a resonance at this supply voltage or a feedback due to the reference voltages. There was no time

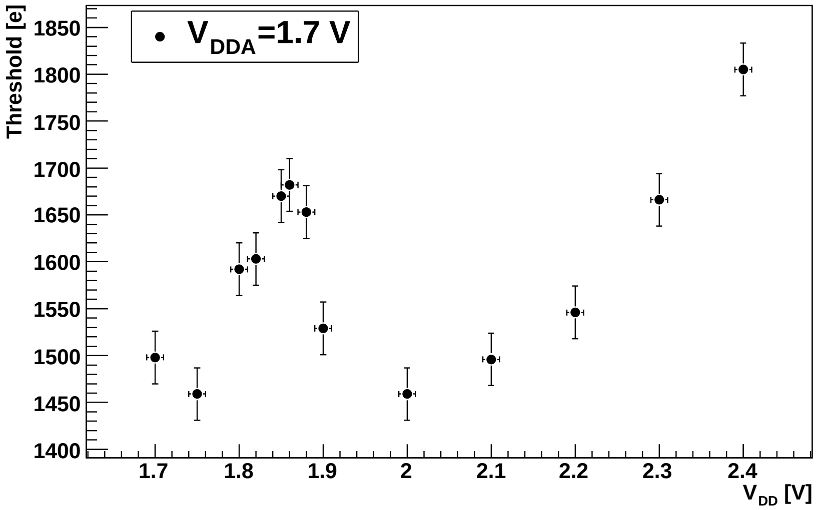

Figure 5.2: Dependency of the minimum threshold on the digital voltage V_{DD} without sensor.

to take this further into account.
Values for the digital supply voltage between 2.0 V and 2.1 V seem to be the best to avoid the peak and the increased crosstalk.

Figures 5.3 and 5.4 show the measurements with sensor. The data of the variation of the analogue supply current is again fitted with a constant. There is a good agreement between the data and the fit. The influence of the analogue supply voltage on the minimum threshold is smaller than for the measurement without sensor. The variation of the measurement with the digital supply voltage is also smaller than without sensor. The peak is not as distinctive as without sensor but there might be one. At least there is a change in the gradient. This could be caused by the same reasons as without sensor. For higher voltages the minimum threshold increases like for the measurement without sensor due to increased crosstalk.

5.2 Feedback Current

There is a known effect on the threshold if the feedback current is varied. The preamplifier needs a finite rising time (some 10 ns). The feedback current discharges the capacitor but does not wait until the whole charge is collected. Hence a part of the signal gets lost. The higher the feedback current is, the more signal gets

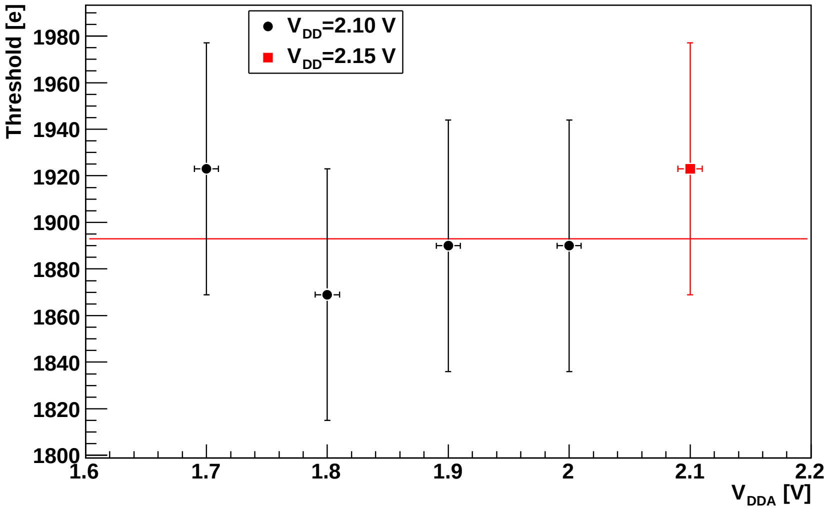

Figure 5.3: Dependency of the minimum threshold on the analogue voltage V_{DDA} with sensor.

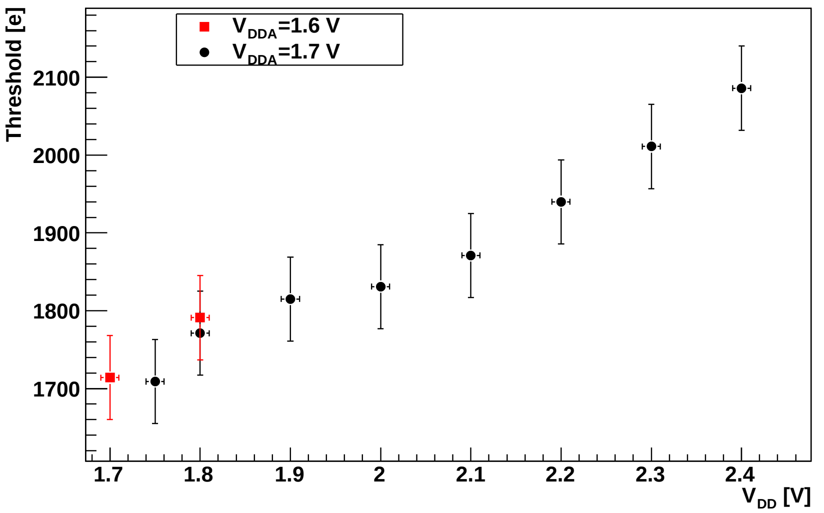

Figure 5.4: Dependency of the minimum threshold on the digital voltage V_{DD} with sensor.

lost. It follows that, if the injected charge stays constant, the height of the signal at the output of the preamplifier decreases if the feedback current increases. It seems as if the threshold is increased, but the threshold of the discriminator is the same, because the TDAC settings were not changed [13].
It is follows that

$$Thr_{\text{measure}} = Thr_0 + Q_{\text{loss}}, \tag{5.1}$$

where Thr_{measure} is the measured threshold in electron charges, Thr_0 is the threshold at $I_F = 0$ and Q_{loss} is proportional to I_F, $Q_{\text{loss}} = t \cdot I_F$ where t is the time that the preamplifier needs to peak. This is a linear behaviour, because the capacitor is discharged with a constant current.

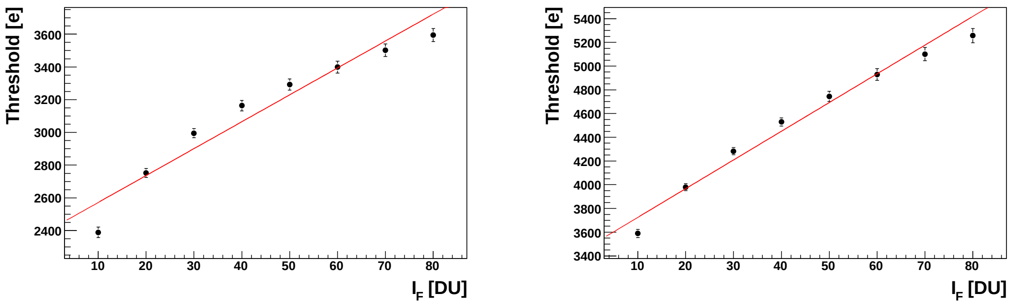

Figure 5.5: Dependency of the standard threshold on the feedback current I_F without sensor (left) and with sensor (right).

In Figure 5.5 the increase of the standard threshold can be seen. The data was fitted with Function 5.1. The rise time t and the threshold charge $Q_{\text{threshold}}$ are estimated:

$$\begin{aligned} t_{\text{exp}} &= (16.4 \pm 0.5)\ \frac{e}{\text{DU}} \qquad Q_{\text{threshold}} = (2407 \pm 24)\ e \quad \text{without sensor,} \\ t_{\text{exp}} &= (24.1 \pm 0.7)\ \frac{e}{\text{DU}} \qquad Q_{\text{threshold}} = (3482 \pm 28)\ e \quad \text{with sensor.} \end{aligned}$$

The fit does not match the data completely, but the signal was assumed to have triangular form. If the signal is observed on an oscilloscope, it is more round.
The difference between the chip without and with sensor is due to the sensor, which acts as an additional capacity. The charge is injected between the sensor and the preamplifier and thus the sensor is charged.

For a check of consistency the experimental rising time t_{exp} is compared with the rising time shown on the oscilloscope $t_{\mathrm{scope}} \approx 10 - 70$ ns. Therefore the feedback current in DAC units has to be converted into A. The current can be measured directly, only reduced by a factor 8000 on the testpad pin (MonDAC) (see [11]). The conversion factor is $c = (14.550 \pm 0.003)\ \frac{\mathrm{ns}}{\mathrm{DU}}$. The experimental rising times are

$$\begin{aligned} t_{\mathrm{exp}} &= (18.0 \pm 0.6)\ \mathrm{ns} \quad \text{without sensor,} \\ t_{\mathrm{exp}} &= (26.5 \pm 0.8)\ \mathrm{ns} \quad \text{with sensor.} \end{aligned}$$

This is consistent to the predicted values.

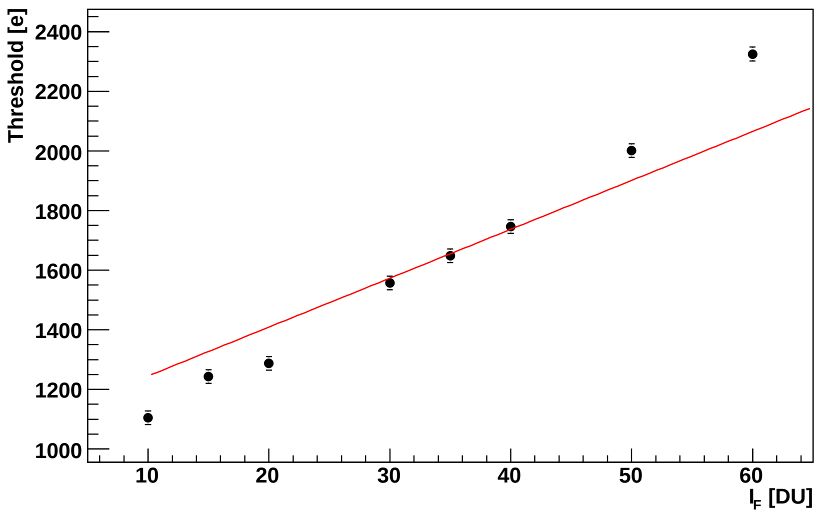

Figure 5.6: Dependency of the minimum threshold on the feedback current I_F without sensor.

Figure 5.6 and Figure 5.7 show the dependency of the minimum threshold on the feedback current I_F. The minimum threshold increases also with the current. To analyse if the behaviour is caused by the effect described above, the data was fitted with the same formula. Only the rising time was fixed to the values above. The fit

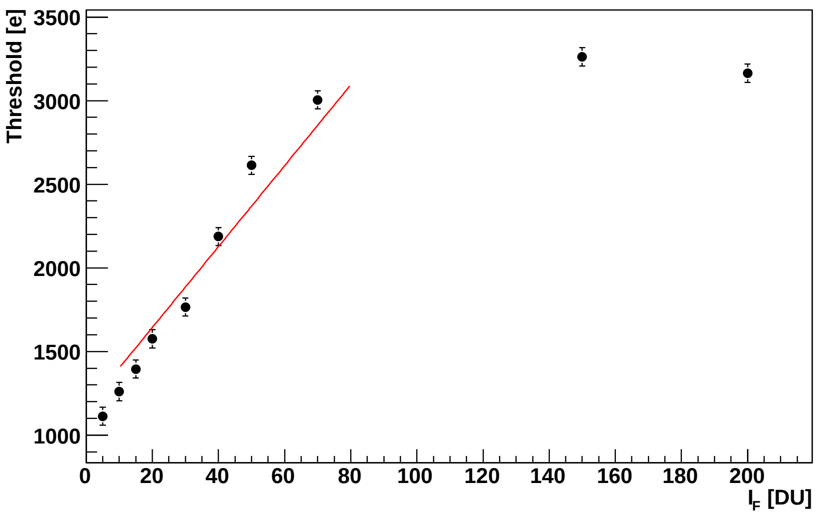

Figure 5.7: Dependency of the minimum threshold on the feedback current I_F with sensor.

results are:

$$Q_{\text{threshold}} = (1081 \pm \ 8)\ e \quad \text{without sensor,}$$
$$Q_{\text{threshold}} = (1159 \pm 20)\ e \quad \text{with sensor.}$$

The agreement between the data and the fit is not good. For lower feedback currents the data are below the fit and for higher feedback current they are above. Thus the feedback current changes the minimum threshold in the same way the threshold does, but there are further effects. The feedback current changes the gradient of the falling edge of the signal (see figure 2.5). Hence the probability that a signal, which is below the threshold, gets due to the noise above the threshold increases for small feedback current. The minimum threshold decreases.

For high I_F currents, the threshold stops changing and saturates. It seems as if the influence of the feedback current on the minimum threshold decreases. It could be that the capacitor can not be discharged faster.

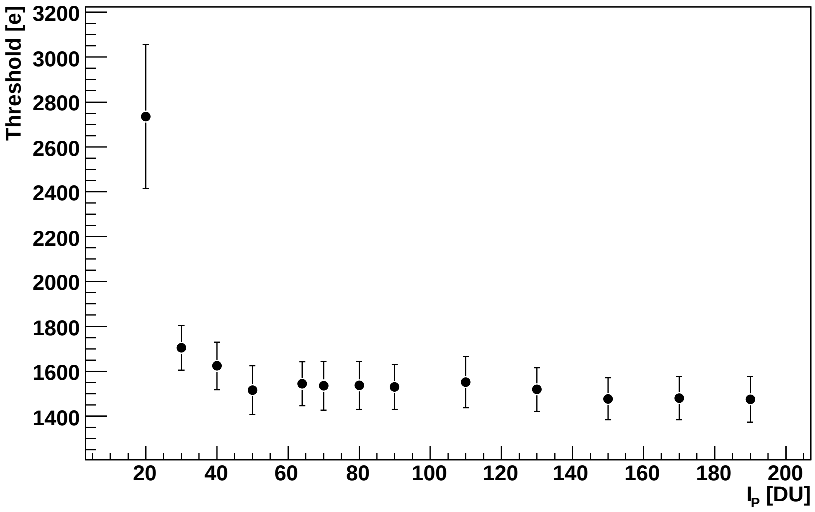

Figure 5.8: Dependency of the minimum threshold on the preamplifier current I_P without sensor.

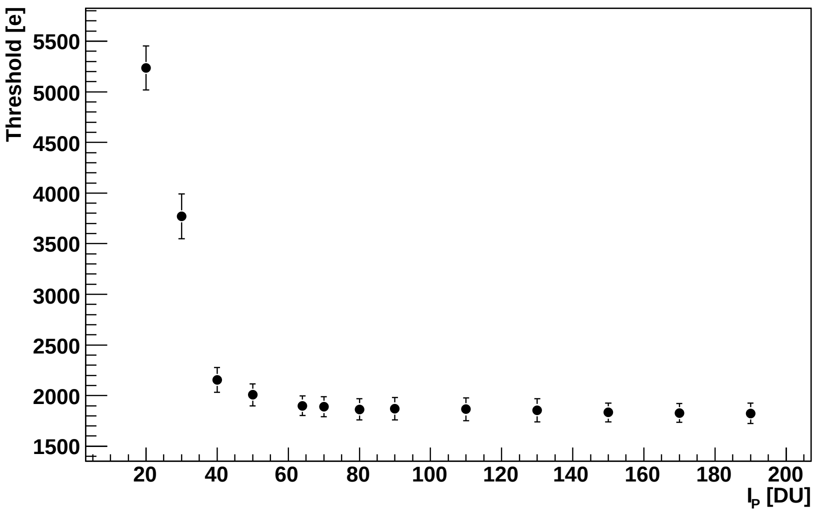

Figure 5.9: Dependency of the minimum threshold on the preamplifier current I_P with sensor.

5.3 Preamplifier Current

The behaviour for the chip with and without sensor is similar except for the value of the minimum threshold. For preamplifier currents between 40 DU and 190 DU the minimum threshold is constant (see Figures 5.8 and 5.9). The analogue current increases because the amplifier current increases. If the current gets too low, the preamplifier stops working properly. At higher I_P, the analogue current gets so high that the measurements were stopped in order to avoid damage on the chip.
The effect that the threshold increases for low I_P is not due to the incremental TDAC scan. Even with a tuned chip at 3000 e the threshold increases if the preamplifier current decreases. The rise time of the signal is influenced by I_P. The smaller the amplifier current gets, the larger gets the rise time. Together with the rising time increases the lost charge due to the ballistic deficit (see Section 5.2) and the minimum threshold increases.

5.4 Amplifier Current

The dependency of the threshold on the amplifier current I_{P2} is shown in Figure 5.10 for a chip without sensor and in Figure 5.11 for a chip with sensor.
A variation of the amplifier current I_{P2} does not decrease the minimum threshold. It is constant for a current between 40 DU - 90 DU. For low I_{P2} the minimum threshold increases because the amplifier stops working properly.
For higher currents the minimum threshold increases again. At $I_{P2} = 100$ DU there are some pixels with a even higher minimum threshold. The analogue current decreases for high I_{P2} again. This is caused by a movement of the operating point of the transistors.
For further information, the amplifier signal was followed on the oscilloscope. The resolution was not good but the peak of the signal stayed in one position. The offset of the signal increases with I_{P2}. Between 50 DU - 70 DU the signal is the largest. At small currents ($I_{P2} < (10 - 20)$ DU) no signal can be seen. At larger currents ($I_{P2} > (90 - 110)$ DU) the amplitude of the signal decreases because the offset increases.

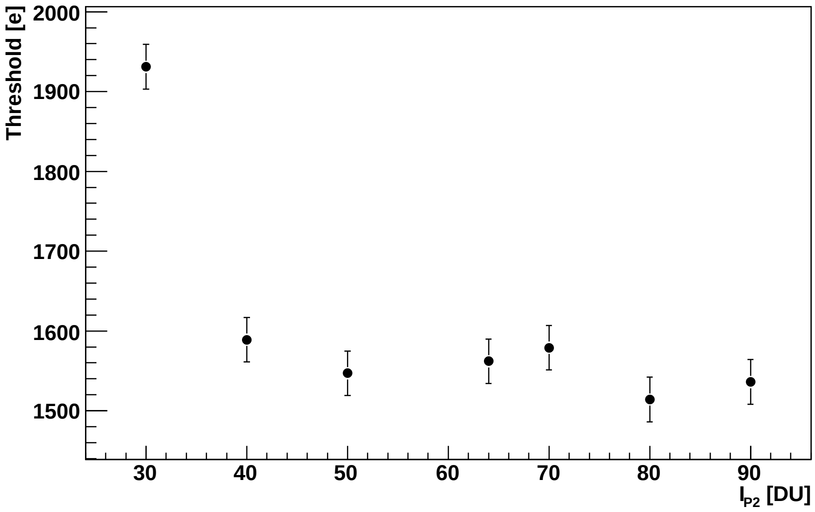

Figure 5.10: Dependency of the minimum threshold on the amplifier current I_{P2} without sensor.

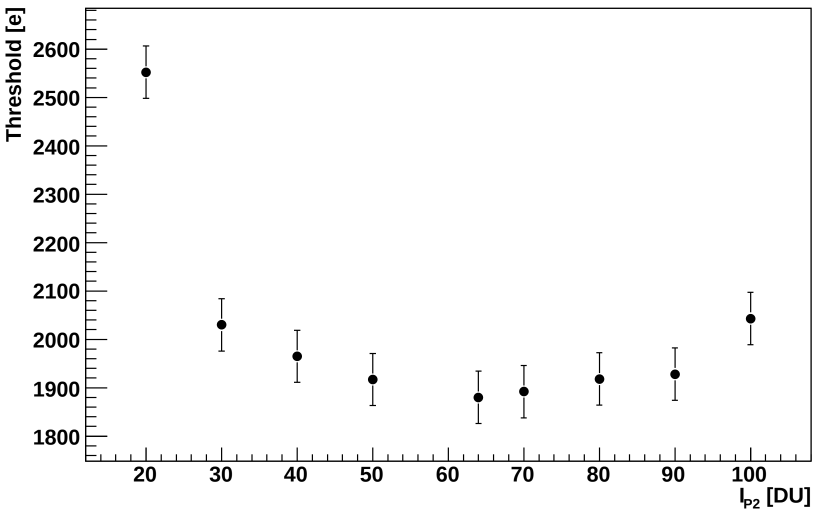

Figure 5.11: Dependency of the minimum threshold on the amplifier current I_{P2} with sensor.

5.5 Discriminator Current

Figure 5.12 and 5.13 show the minimum threshold versus the discriminator current I_D without and with sensor. For the chip without sensor the threshold stays constant below $I_D < 80$ DU. Above that, the minimum threshold increases. If the chip has a sensor, the minimum threshold increases for $I_D \geq 100$ DU. The analogue current increases with the discriminator current. Because of this, the measurement is stopped at higher currents, because too high currents can damage the chip. The minimum threshold increases for higher currents, because there is more noise.

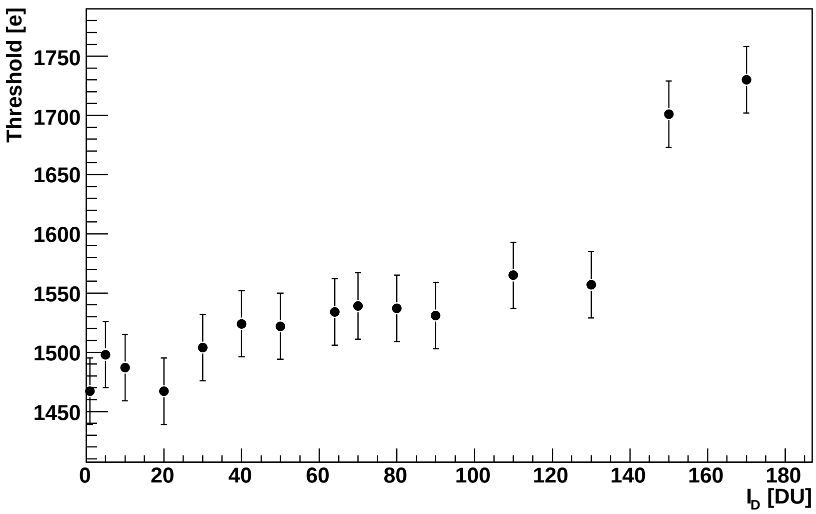

Figure 5.12: Minimum threshold versus discriminator current I_D without sensor.

5.6 GDAC

The GDAC changes the threshold globally. For the measurements during this thesis always the same GDAC values are used (see Table 5.1). To check if the incremental TDAC scan works as expected the GDAC values are varied. If the scan works independently from the threshold at the start point, the minimum threshold is not supposed to vary. Figure 5.14 and 5.15 show the data. The error for the measurements is the error of the measurement method, which is estimated as described at the beginning of this chapter (Chapter 5).

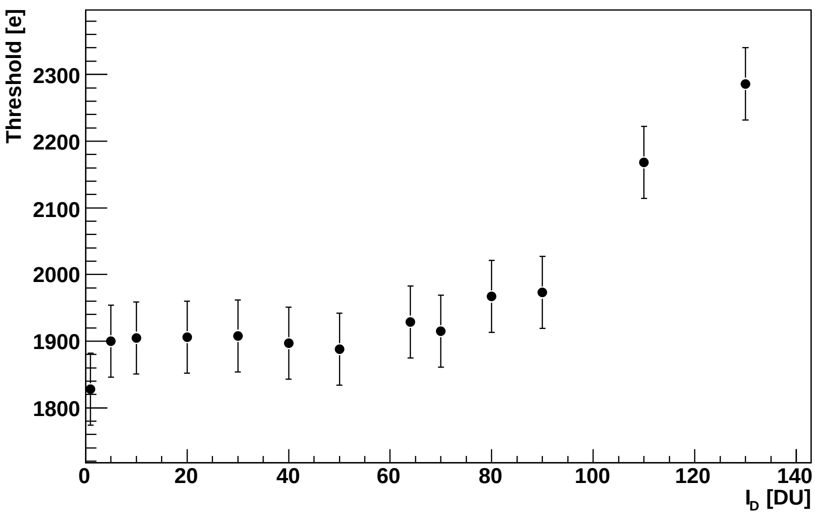

Figure 5.13: Minimum threshold versus discriminator current I_D with sensor.

The data are fitted with a constant function and χ^2 is regarded.

$$\chi^2 = 3.21 \quad n = 6 \quad \text{without sensor,}$$
$$\chi^2 = 1.43 \quad n = 8 \quad \text{with sensor,}$$

where n is the degree of freedom. With χ^2 and n the probability p that there is a larger χ^2 value can be calculated.

$$p = 78.22\% \quad \text{without sensor}$$
$$p = 99.37\% \quad \text{with sensor}$$

If $p = 50\%$ the χ^2 is most probable and the prediction that the behaviour is constant agrees best with the data. The determined values confirm that the data only vary around a mean value. The agreement for the measurement without sensor is better than the measurement with sensor, because the value is closer to 50%. The GDAC does not affect the scan.
To stress this the mean values of TDAC for GDAC=4 DU and GDAC=16 DU were checked. It is expected that if the GDAC increases the mean value of TDAC decreases to get the same minimum threshold. This is confirmed by the data. Furthermore, the TDAC values do not get below 10 DU, where the threshold does not behave linearly with respect to the TDAC.

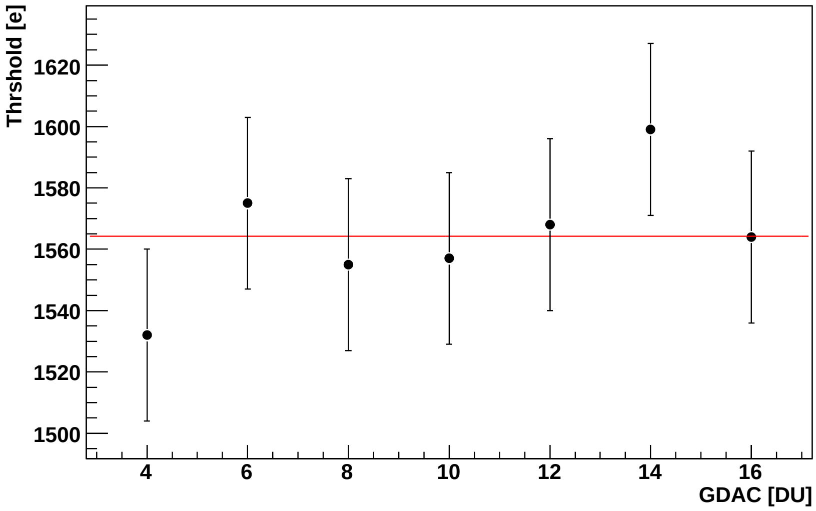

Figure 5.14: Dependency of the minimum threshold on GDAC without sensor.

5.7 Masks

The number of pixels into which charge is injected simultaneously is decreased. Charge cannot be injected into every pixel at the same time, because this would be too much data for the read-out. Furthermore, the crosstalk increases, but this is only a small effect.

The arrangement of the pixel in which charge is injected at the same time is called a mask. A mask with step size x has to be repeated x times to inject charge into every pixel. The design of the injections is column by column in a wiggly line. The first step size, which can be arranged well, is 32. This is the common step size. The different tested step sizes are 32, 40, 64, 80, and 160. The masks with 320 and 2880 were damaged at the time of the thesis.

Figures 5.16 and 5.17 show the results. From the 32 step mask to the 40 step mask the minimum threshold decreses, because the digital crosstalk decreases. There could be a minimum at mask 40. Then the minimum threshold increases and comes soon to a saturation. This process is not understood. There could be a coherent process of the pixels. To prove that masks with bigger step size would be needed.

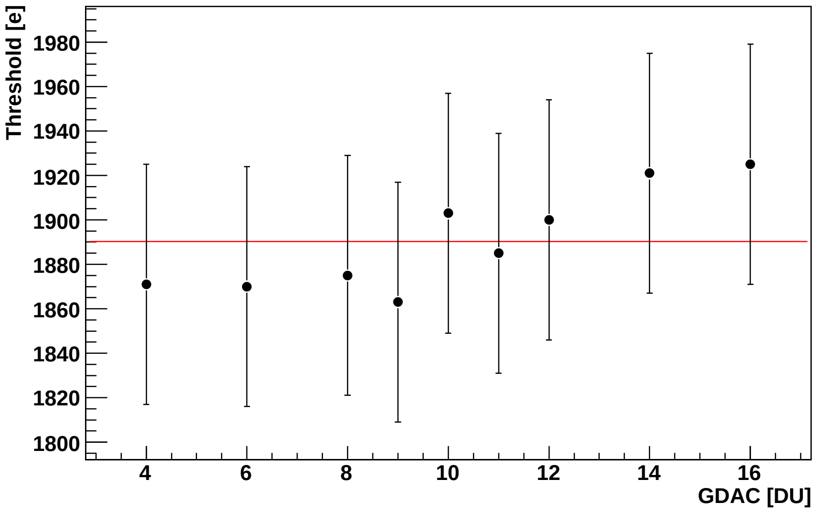

Figure 5.15: Dependency of the minimum threshold on GDAC with sensor.

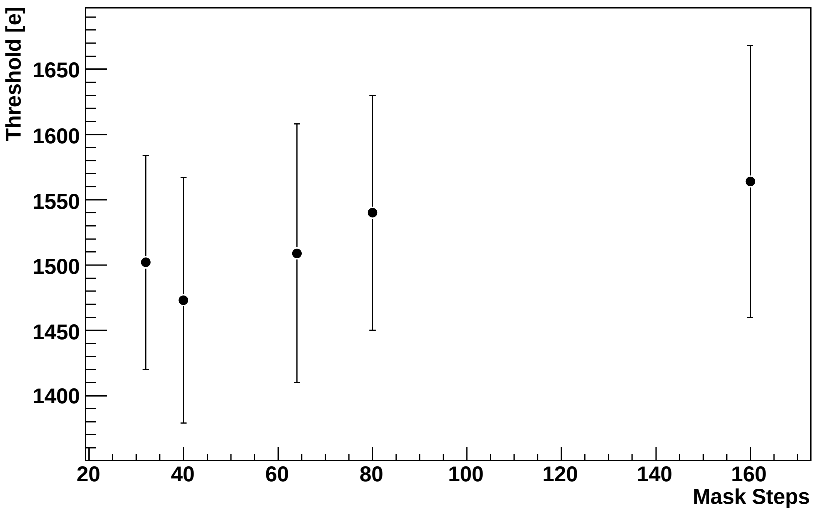

Figure 5.16: Dependency of the minimum threshold on mask steps without sensor.

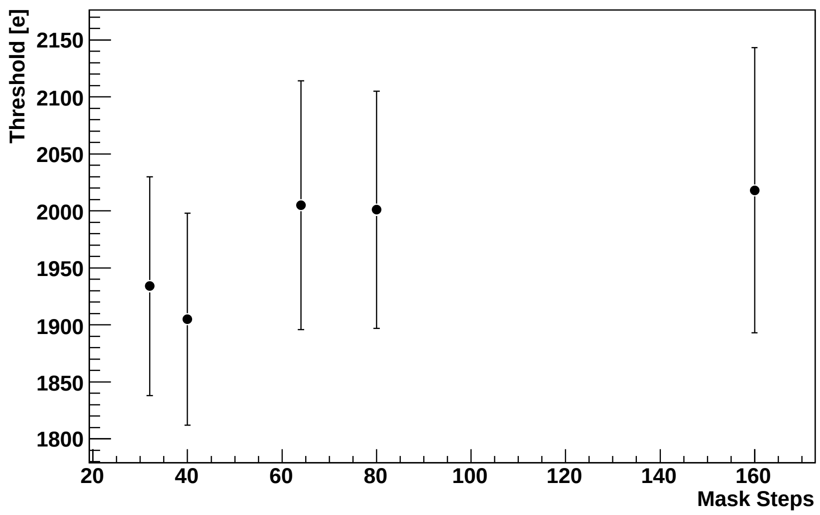

Figure 5.17: Dependency of the minimum threshold on mask steps with sensor.

5.8 Grounding

The digital and the analogue circuit have seperate supply voltages which are in reference to different grounds. These two grounds are connected on the single chip card. It was tested if the minimum threshold decreases if the chip substrate is grounded and the digital and the analogue ground are connected on different positions.
Therefore a new chip without sensor is attached to a single chip card with conductive glue. The places where the analogue and the digital ground are connected are varied (see Table 5.2).

place of connection	threshold [e]
power supply	1792 ± 28
single chip card	1473 ± 28
supply voltage & single chip card	1463 ± 28
no connection	–
grounded chip	1451 ± 28

Table 5.2: Variation of the place of connection of the two different grounds.

It can be seen that the grounds have to be connected at some point. If they are not connected the signal can not be read out. The difference between logical one and logical zero would be too small, because the grounds have an offset towards each

other.
If the connection is on the power supply, there is a large area for a ground loop. Thus there is a good antenna and there is electromagnetic pick-up. Because of this there is more noise, which increases the minimum threshold. If there is a connection on the board, the chip has the lowest minimum threshold.
With the conductive glue the chip was glued on the single chip card and the chip substrate was grounded to the digital ground. There is no variation compared to the normal fluctuation.

6 Conclusions

6.1 Minimum Threshold Measurements

Three methods were tested to find the minimum threshold. The hitbus method is very instable. The hit rate is strongly influenced by external factors like temperature and time of a measurement.
The TDAC tune methods works well for standard thresholds. If the threshold is below 2000 e there are some 100 pixels lost which means that their thresholds develop in the wrong direction.
Finally the incremental TDAC scan works very reliably and is stable. Due to the adjustable cuts the method is flexible for changes. That means for the aim of the thesis, namely decreasing the minimum threshold, that improvements due to different configurations can be discovered.

6.2 Different Approches to the Minimum Threshold

At first, several chip parameters were varied to decrease the minimum threshold. There was only one parameter, the feedback current, found that achieves this aim. The other parameter did not decrease the minimum threshold, but some different effects were found.
The two supply voltages were varied. If the analogue supply voltage is changed fluctuations around a mean value were discovered. There are reference voltages generated by the supply voltages, which could cause effects that are not understood. Even if the dependency of the minimum threshold on the digital supply voltage is regarded, there appears a peak at lower voltages, which could also be caused by the effects of the reference voltages.
The currents of the two amplifiers and the discriminator were also varied. The results for the chips without and with sensor are similar.
The feedback current shows the same dependency on the minimum threshold as

on a standard threshold and some more effects. The minimum threshold decreases with the feedback current. But with a smaller feedback current the capacitor is discharged slower. It has to pointed out that the next event is not missed. A good balance between low threshold and read-out speed has to be found.
The preamplifier and the amplifier current have no influence on the minimum threshold. The discriminator current has a small influence on the minimum threshold but only to larger minimum thresholds, because of the electronic noise that increases with higher currents. For currents up to about 80 DU, the minimum threshold is constant.
To check the reliability of the incremental TDAC scan, the GDAC was varied. This causes a variation of the start configuration of the chips. The result is that the minimum threshold stays constant even for different initial thresholds.
The variation of the connection position of the digital and the analogue ground affected the minimum threshold in the wrong direction. The grounds have to be connected on the single chip card in order to avoid feedback and thus an increase of the minimum threshold.
The number of pixels in which charge is injected is the most promising parameter to lower minimum threshold. Unfortunately, the large mask step sizes did not work during the thesis. The problem is solved now and this measurement could be completed soon.
Furthermore, the test needs higher statistics to be able to give a reliable conlusion on the fluctuations. It could also be interesting to see the impact of a variation of two parameters at the same time.

Bibliography

[1] *The ATLAS Experiment*, http://www.atlas.ch/photos/

[2] P. Sícho, *SLHC upgrade plans for the ATLAS pixel detector* Nuclear Instr. Meth. A 607 (2006) 31-34

[3] G. Aad etal, *ATLAS pixel detector electronics and sensors*, 2008 JINST 3 P07007 (2008)

[4] J. Große-Knetter, *Vertex Measurement at a Hadron Collider - The ATLAS Pixel Detector*, BONN-IR-2008-04 (2008)

[5] W.R. Leo, *Techniques for Nuclear and Particle Physics Experiments - A How-to Approch*, Springer-Verlag (1994)

[6] I. Peric etal, *The FEI3 readout chip for the ATLAS pixel detector*, Nuclear Instr. Meth. A 565 (2006) 178-187

[7] T. Flick, *Studies on the Optical Readout for the ATLAS Pixel Detector*, WUB-DIS-2006-05 (2006)

[8] M. Backhaus, *Development of an USB-based test system for the FE-I3 readout chips of the ATLAS pixel detector and Noise Occupancy Studies*, BONN-IB-2009-14 (2009)

[9] *USBPix System documentation* http://icwiki.physik.uni-bonn.de/twiki/bin/view/Systems/UsbPix

[10] J. Weingarten, *System Test and Noise Performance Studies at the ATLAS Pixel Detector*, BONN-IR-2007-10 (2007)

[11] K. Einsweiler, *ATLAS On-detector Electronics Architecture*, Draft V3.0 (2003)

[12] P. Behara etal, *Threshold Tuning of the ATLAS Pixel Detector*, ATL-COM-INDET-2010-044 (2010)

[13] M. Keil, *Pixeldetektoren aus Silizium und CVD-Diamant zum Teilchennachweis in ATLAS bei LHC*, BONN-IR-2001-13 (2001)

Danksagung

Ich möchte mich ganz herzlich bei allen Bedanken, die zum Erstellen dieser Arbeit beigetragen haben.

Ganz besonders möchte ich mich bei Jörn Große-Knetter bedanken, den ich immer mit meine Fragen löchern durfte und der mir stets Rede und Antwort gestanden hat.
Auch Matthias George und Jens Weingarten danke ich für die Hilfe und vor allem für das Korrekturlesen der Arbeit.
Danke auch an Nina Krieger und Benjamin von Ardenne für die Hilfe bei technischen Fragen und ohne die die Arbeit im Labor nicht so lustig gewesen wäre.
Schließlich danke ich allen Institutmitglieder des II. Physikalischen Instituts der Universität Göttingen, dass sie mich in das Institutsleben eingeführt haben.

Auch Herrn Prof. Dr. Quadt möchte ich danken für die Möglichkeit, dass ich eine Bachelorarbeit zu einem Teil des ATLAS Projektes schreiben durfte.

Nicht zuletzt ein Dankeschön an meine Eltern und meinen Freund, dass sie mir immer Kraft geben und mich unterstützen, wo sie nur können.

Vielen Dank auch an alle, die ich nicht aufgezählt habe und die mir weitergeholfen haben!

Erklärung nach §13(8) der Prüfungsordnung für den Bachelor-Studiengang Physik und den Master-Studiengang Physik an der Universität Göttingen:

Hiermit erkläre ich, dass ich diese Abschlussarbeit selbständig verfasst habe, keine anderen als die angegebenen Quellen und Hilfsmittel benutzt habe und alle Stellen, die wörtlich oder sinngemäß aus veröffentlichten Schriften entnommen wurden, als solche kenntlich gemacht habe.
Darüberhinaus erkläre ich, dass diese Abschlussarbeit nicht, auch nicht auszugsweise, im Rahmen einer nichtbestandenen Prüfung an dieser oder einer anderen Hochschule eingereicht wurde.

Göttingen, den November 30, 2010

(Julia Rieger)